# TD-GIN: Token-level Dynamic Graph-Interactive Network for Joint Multiple Intent Detection and Slot Filling

**Libo Qin, Xiao Xu, Wanxiang Che**,[*] **Ting Liu**
Research Center for Social Computing and Information Retrieval
Harbin Institute of Technology, China
{lbqin,xxu,car,tliu}@ir.hit.edu.cn

## Abstract

Intent detection and slot filling are two main tasks for building a spoken language understanding (SLU) system. Currently, most work on SLU have focused on the single intent scenario, and paid less attention into the multi-intent scenario, which commonly exists in real-world scenarios. In addition, multi-intent SLU faces an unique challenges: how to effectively incorporate multiple intents information to guide the slot prediction. In this paper, we propose a Token-level Dynamic Graph-Interactive Network (TD-GIN) for joint multiple intent detection and slot filling, where we model the interaction between multiple intents and each token slot in a unified graph architecture. With graph interaction mechanism, our framework has the advantage to automatically extract the relevant intents information to guide each token slot prediction, making a fine-grained intent information integration for the token-level slot prediction. Experiments on two multi-intent datasets show that our model achieves the state-of-the-art performance and outperforms other previous methods by a large margin. Comprehensive analysis empirically shows that our framework successfully captures multiple relevant intents information to improve the SLU performance.

## 1 Introduction

Spoken language understanding (SLU) (Young et al., 2013) is a core component of task-oriented dialog systems. It consists of two typical subtasks, intent detection and slot filling (Tur and De Mori, 2011). Take the utterance "*Please play Happy Birthday*" for example, the intent detection can be seen as a classification task to classify the intent label (*i.e.*, PlayMusic) while the slot filling can be treated as a sequence labeling task to predict the slot label sequence (*i.e.*, O, O, B-music,

I-music). Since slots highly depend on the intent information, dominant SLU systems in the literature (Goo et al., 2018; Li et al., 2018; Xia et al., 2018a; Qin et al., 2019; E et al., 2019; Liu et al., 2019) adopt joint models for the two tasks, which is a direction we follow.

Though achieving promising performances, most prior work just focus on the simple single intent scenario. Their models are trained based on the assumption that each utterance only has one single intent, failing to effectively handle the complex multiple intents settings, which commonly appear in real-world scenarios (Gangadharaiah and Narayanaswamy, 2019). Ideally, when an SLU system meets an utterance with multiple intents, which is shown in Figure 1(a), the model should directly detect its all intents (PlayMusic and AddToPlaylist) that prior single intent SLU system fail to handle. Hence, it's important to consider the multi-intent SLU.

Unlike the prior single intent SLU which can simply concat the utterance's intent to guide slot prediction, multi-intent SLU faces to multiple intents and presents an unique challenges that is worth studying: how to effectively incorporate multiple intents information to lead the slot prediction. To this end, Gangadharaiah and Narayanaswamy (2019) first explored the multi-task framework with slot-gated mechanism (Goo et al., 2018) for joint multiple intents detection and slot filling. Their model simply took an intent's context vector as multiple intents information to leverage it for modeling slot-intent relationships. While this is a direct method for incorporating multiple intents information, it does not offer fine-grained intent information integration for token-level slot filling in the sense that each token is guided with the same complex intents information, which is shown in Figure 1(a). Besides, providing the same intent information for all tokens may introduce ambiguity,
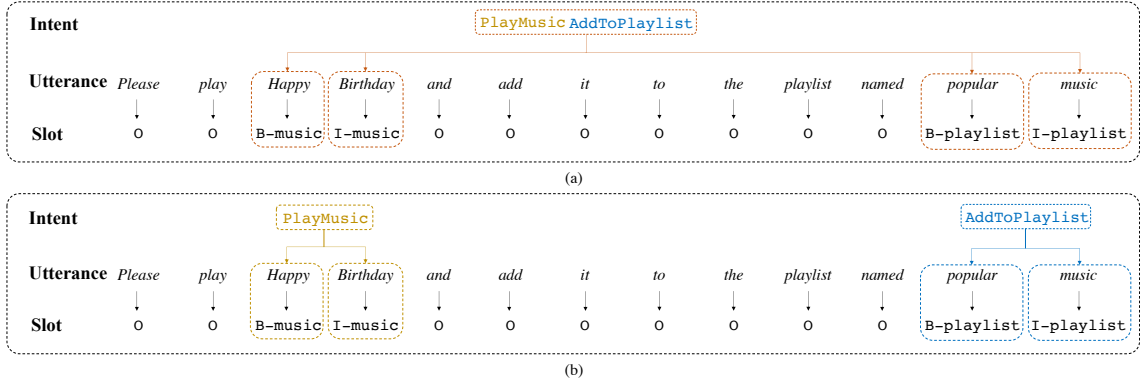
Figure 1: Prior model simply treat multiple intents as an overall intent information (a) vs. our fine-grained multiple intents integration method (b).

where it's hard for each token to capture the related intent information. As shown in Figure 1(b), these tokens "*Happy Birthday*" should focus on the intent "PlayMusic" while tokens "*popular music*" depend on the intent "AddToPlaylist". Thus, different tokens should focus on different intents and it's critical to make a fine-grained intent information integration for the token-level slot prediction.

In this paper, we propose a Token-level Dynamic Graph-Interactive Network (TD-GIN) to address the aforementioned concerns for multi-intent SLU. The core module is a proposed intent-slot interaction graph layer based on each token's hidden state of slot filling decoder and embeddings of predicted multiple intents. In this graph, each token's slot node directly connects all intent nodes to explicitly build the correlation between slot and intents where slot can aggregate the multiple intents information and intent can incorporate the slot information. In contrast to prior work simply incorporate multiple intents information statically where the same intents information are used for guiding all tokens, our intent-slot interaction graph is constructed dynamically with graph attention network over each token. This encourages our model to automatically filter the irrelevant information and capture important intent information, which achieves a fine-grained intents information integration for guiding the token-level slot prediction.

We first conduct experiments on the multi-intent benchmark datasets DSTC4 (Schuster et al., 2019). Then, to verify the generalization of our framework, we empirically construct a large-scale multi-intent datasets MixSNIPS (Coucke et al., 2018). The results of both experiments show the effectiveness of our framework by outperforming the

current state-of-the-art method by a large margin. In addition, our framework achieves the state-of-the-art performance on two public single-intent datasets including ATIS (Tur and De Mori, 2011) and SNIPS (Coucke et al., 2018), which further verifies the generalization of the proposed model.

Our contributions in this work are as follows: 1) We propose to exploit the multiple intents for guiding the slot into an intent-slot interaction graph architecture, aiming to make a fine-grained intent information integration for the token-level slot prediction. To our best knowledge, this is the first investigation in this direction. 2) We propose a token-level dynamic graph-interactive framework with graph attention network, which can automatically aggregate the relevant multiple intents information at token-level. 3) We empirically construct a large-scale multi-intent SLU dataset. The release of it would push forward the research of multi-intent SLU.

## 2 Approach

In this section, we will describe our token-level dynamic graph-interactive framework. The architecture of our framework is demonstrated in Figure 2, which consists of an encoder and two decoders. First, the encoder module uses a shared self-attentive encoder to represent an utterance, which can grasp the shared information between intent detection and slot filling. Then, the intent-detection decoder performs the multi-label classification to detect multiple intents. Finally, we directly leverage the multiple intents information to guide slot prediction dynamically by the proposed token-level intent-slot graph interaction layer. Both intent detection and slot filling are optimized simultaneously via a multi-task learning scheme.
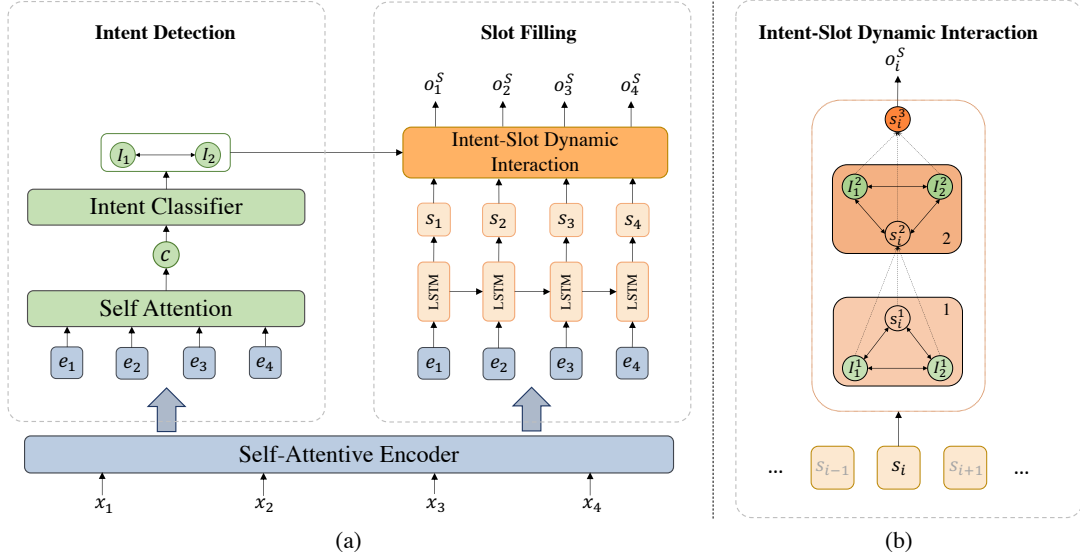
Figure 2: The overflow of model architecture (a) and intent-slot dynamic graph interaction module (b).

## 2.1 Self-Attentive Encoder

In the self-attentive encoder, we use BiLSTM with self-attention mechanism to leverage both advantages of temporal features within word orders and contextual information, which are useful for sequence labeling tasks (Zhong et al., 2018).

**Bidirectional LSTM** A bidirectional LSTM (BiLSTM) (Hochreiter and Schmidhuber, 1997) consists of two LSTM layers. For the input sequence $\{\boldsymbol{x}_1, \boldsymbol{x}_2, \dots, \boldsymbol{x}_T\}$ ($T$ is the number of tokens in the input utterance), the BiLSTM reads it forwardly from $\boldsymbol{x}_1$ to $\boldsymbol{x}_T$ and backwardly from $\boldsymbol{x}_T$ to $\boldsymbol{x}_1$ to produce a series of context-sensitive hidden states $\boldsymbol{H} = \{\boldsymbol{h}_1, \boldsymbol{h}_2, \dots, \boldsymbol{h}_T\}$.

**Self-Attention** In this paper, we follow (Qin et al., 2019) to use a self-attention mechanism over word embedding to capture context-aware features. In this paper, we adopt the self-attention formulation by Vaswani et al. (2017). We first map the matrix of input vectors $\boldsymbol{X} \in \mathbb{R}^{T \times d}$ ($d$ represents the mapped dimension) to queries $\boldsymbol{Q}$, keys $\boldsymbol{K}$ and values $\boldsymbol{V}$ matrices by using different linear projections parameters $\boldsymbol{W}_q, \boldsymbol{W}_k, \boldsymbol{W}_v$: and the attention weight is computed by dot product between $\boldsymbol{Q}$, $\boldsymbol{K}$ and the self-attention output $\boldsymbol{C} \in \mathbb{R}^{T \times d}$ is a weighted sum of values .

$$\boldsymbol{A} = \mathrm{softmax}\left(\frac{\boldsymbol{Q}\boldsymbol{K}^{\top}}{\sqrt{d_k}}\right)\boldsymbol{V}, \qquad (1)$$

where $d_k$ denotes the dimension of keys.

After obtaining the output of self-attention and BiLSTM. We concatenate these two representa-

tions as the final encoding representation:

$$\boldsymbol{E} = [\boldsymbol{H} \,\|\, \boldsymbol{A}], \qquad (2)$$

where $\boldsymbol{E} = \{\boldsymbol{e}_1, \dots, \boldsymbol{e}_T\} \in \mathbb{R}^{T \times 2d}$ and $\|$ is concatenation operation.

## 2.2 Intent Detection Decoder

In this section, we describe the intent detection decoder, which is performed as the multi-label classification problem. After obtaining the sequence self-attentive encoding representations $\boldsymbol{E} = \{\boldsymbol{e}_1, \dots, \boldsymbol{e}_T\}$, we further compute the utterance context vector for intent prediction. In our case, we use a self-attention module (Zhong et al., 2018; Goo et al., 2018) to compute relevant attention context for intent detection. The context attention score and intent context vector can be calculated as:

$$p_t = \mathrm{softmax}(\boldsymbol{W}_e\,\boldsymbol{e}_t + \boldsymbol{b}), \qquad (3)$$

$$\boldsymbol{c} = \sum_t p_t \boldsymbol{e}_t, \qquad (4)$$

where $\boldsymbol{W}_e \in \mathbb{R}^{1 \times 2d}$ is the trainable parameters, $p_t$ is the corresponding normalized self-attention score and $\boldsymbol{c}$ is the weighted sum of each element $\boldsymbol{e}_t$, representing the utterance context information.

Then the context vector $\boldsymbol{c}$ is utilized for intent detection:

$$\boldsymbol{y}^I = \mathrm{sigmoid}(\boldsymbol{W}_c\,\boldsymbol{c} + \boldsymbol{b}), \qquad (5)$$

where $\boldsymbol{W}_c$ are trainable parameters of the intent decoder, $\boldsymbol{y}^I = \{y_1^I, \dots, y_{N_I}^I\}$ is the intent output

of the utterance and $N_I$ is the number of single intent labels.

During inference, we predict intents index $\boldsymbol{I}$ = $\{I_1, \ldots, I_n\}$ and $I_i$ represents probability $y_{I_i}^I$ greater than $t_u$, where $0 < t_u < 1.0$ is a hyperparameter tuned using the validation set. [1] For example, if the $\boldsymbol{y}^I = \{0.9, 0.3, 0.6, 0.7, 0.2\}$ and the $t_u$ is 0.5, we predict intents $\boldsymbol{I} = \{0, 2, 3\}$, where index starts from 0.

### 2.3 Intent-Slot Dynamic Interaction Graph for Slot Filling

In this paper, one of the core contribution is dynamically leverage multiple intents to guide the slot prediction. In particular, we adopt the graph attention network (GAT) (Veličković et al., 2017) to model the interaction between intents and slot to automatically capture relevant intents for slot.

In this section, we first describe the vanilla graph attention network. Then, we show how to directly leverage multiple intents information for slot prediction with intent-slot graph interaction layer.

**Vanilla Graph Attention Network**  For a given graph with $N$ nodes, one-layer GAT take the initial node features $\tilde{\boldsymbol{H}} = \{\tilde{\boldsymbol{h}}_1, \ldots, \tilde{\boldsymbol{h}}_N\}, \tilde{\boldsymbol{h}}_n \in \mathbb{R}^F$ as input, aiming at producing more abstract representation (of probably different cardinality $F'$), $\tilde{\boldsymbol{H}}' = \{\tilde{\boldsymbol{h}}_1', \ldots, \tilde{\boldsymbol{h}}_N'\}, \tilde{\boldsymbol{h}}_n' \in \mathbb{R}^{F'}$, as its output. The graph attention operated on the node representation can be written as:

$$\mathcal{F}(\tilde{\boldsymbol{h}}_i, \tilde{\boldsymbol{h}}_j) = \text{LeakyReLU}\left(\mathbf{a}^\top [\boldsymbol{W}_h \tilde{\boldsymbol{h}}_i \| \boldsymbol{W}_h \tilde{\boldsymbol{h}}_j]\right),$$

$$\alpha_{ij} = \frac{\exp(\mathcal{F}(\tilde{\boldsymbol{h}}_i, \tilde{\boldsymbol{h}}_j))}{\sum_{j' \in \mathcal{N}_i} \exp(\mathcal{F}(\tilde{\boldsymbol{h}}_i, \tilde{\boldsymbol{h}}_{j'}))},$$

$$\tilde{\boldsymbol{h}}_i' = \sigma\Big(\sum_{j \in \mathcal{N}_i} \alpha_{ij} \boldsymbol{W}_h \tilde{\boldsymbol{h}}_j\Big),$$

(6)

where $\mathcal{N}_i$ is the first-order neighbors of node $i$ (including $i$) in the graph, $\boldsymbol{W}_h \in \mathbb{R}^{F' \times F}$ and $\mathbf{a} \in \mathbb{R}^{2F'}$ is the trainable weight matrix, $\alpha_{ij}$ is the normalized attention weight denoting the importance of each $h_j$ to $h_i$ and $\sigma$ represents the non-linearity activation function.

GAT inject the graph structure into the mechanism by performing *masked attention*, i.e, GAT only compute $\mathcal{F}(\tilde{\boldsymbol{h}}_i, \tilde{\boldsymbol{h}}_j)$ for nodes $j \in \mathcal{N}_i$. To stabilize the learning process of self-attention, GAT extend the above mechanism to employ *multi-head*

*attention* from Vaswani et al. (2017):

$$\tilde{\boldsymbol{h}}_i' = \mathop{\Big\|}_{k=1}^K \sigma\Big(\sum_{j \in \mathcal{N}_i} \alpha_{ij}^k \boldsymbol{W}_h^k \tilde{\boldsymbol{h}}_j\Big),$$

(7)

where $\alpha_{ij}^k$ is the normalized attention weight computed by the $k$-th function $\mathcal{F}_k$, $\|$ is concatenation operation and $K$ is the number of heads. Thus, the output $\tilde{\boldsymbol{h}}_n'$ will consists of $KF'$ features in the middle layers and the final prediction layer will employ averaging instead of concatenation to get the final prediction results.

**Intent-Slot Dynamic Interaction for Slot Prediction**  We use a unidirectional LSTM as the slot filling decoder. At each decoding step $t$, the decoder state $\boldsymbol{s}_t$ is calculated by previous decoder state $\boldsymbol{s}_{t-1}$, the previous emitted slot label distribution $\boldsymbol{y}_{t-1}^S$ and the aligned encoder hidden state $\boldsymbol{e}_t$:

$$\boldsymbol{s}_t = \text{LSTM}\left(\boldsymbol{s}_{t-1}, \boldsymbol{y}_{t-1}^S, \boldsymbol{e}_t\right).$$

(8)

Instead of directly utilizing the $\boldsymbol{s}_t$ to predict the slot label, we build a graphic structure named intent-slot graph interaction to explicitly leverage multiple intents information to guide the $t$-th slot prediction. In this graph, the slot hidden state at $t$ time step is $\boldsymbol{s}_t$ and predicted multiple intents information $\boldsymbol{I} = \{I_1, \ldots, I_n\}$, where $n$ denotes the number of predicted intents, are used as the initialized representations at $t$ time step $\tilde{\boldsymbol{H}}^{[0,t]} = \{\boldsymbol{s}_t, \phi^{emb}(I_1), \ldots, \phi^{emb}(I_n)\} \in R^{(n+1) \times d}$, where $d$ represents the dimension of vertice representation and $\phi^{emb}(\cdot)$ represents the embedding matrix of intents. In addition, each predicted intents connect each other to consider their mutual interaction because all of them express the same utterance's intent.

For convenience, we use $\tilde{\boldsymbol{h}}_i^{[l,t]}$ to represent node $i$ in the $l$-th layer of the graph consisting of the decoder state node and predicted intent nodes. $\tilde{\boldsymbol{h}}_0^{[l,t]}$ is the slot hidden state representation in the $l$-th layer. To explicitly leverage the multiple intents information, the slot hidden state node directly connect all predicted intents and the node representation in the $l$-th layer can be calculated as:

$$\tilde{\boldsymbol{h}}_i^{[l,t]} = \sigma\Big(\sum_{j \in \mathcal{N}_i} \alpha_{ij}^{[l,t]} \boldsymbol{W}_h^{[l]} \tilde{\boldsymbol{h}}_j^{[l-1,t]}\Big),$$

(9)

where $\mathcal{N}_i$ represents the first-order neighbors of node $i$, *i.e.*, the decoder state node and the predicted intent nodes, and the update process of all node

---

[1] In our experiments, we set $t_u$ as 0.5.

representations can be calculated by Equation 6, 7 and 9.

With $L$-layer intent-slot graph attention interaction, we obtain the final slot hidden state representation $\tilde{\boldsymbol{h}}_0^{[L,t]}$ at $t$ time step as $t$-th token's slot filling feature $\tilde{\boldsymbol{s}}_t$, which dynamically capture important intents information at token-level. The slot filling feature $\tilde{\boldsymbol{s}}_t$ is utilized for slot filling:

$$\boldsymbol{y}_t^S = \mathrm{softmax}\left(\boldsymbol{W}_s \tilde{\boldsymbol{s}}_t\right), \qquad (10)$$

$$o_t^S = \mathrm{argmax}(\boldsymbol{y}_t^S), \qquad (11)$$

where $o_t^S$ is the slot label of the $t$-th word in the utterance.

## 2.4 Multi-Task Training

We adopt a joint model to consider the two tasks and update parameters by joint optimizing. The intent detection objection can be formulated as:

$$\mathcal{L}_1 \triangleq -\sum_{k=1}^{N_I} \left(\hat{y}_k^I \log\left(y_k^I\right) + \left(1 - \hat{y}_k^I\right) \log\left(1 - y_k^I\right)\right) \cdot \qquad (12)$$

Similarly, the slot filling task objection is defined as:

$$\mathcal{L}_2 \triangleq -\sum_{i=1}^{M} \sum_{j=1}^{N_S} \hat{y}_i^{(j,S)} \log\left(y_i^{(j,S)}\right), \qquad (13)$$

where $N_I$ is the number of single intent labels, $N_S$ is the number of semantic labels and $M$ is the number of words in an utterance. The final joint objective is formulated as:

$$\mathcal{L} = \alpha_1 \mathcal{L}_1 + \alpha_2 \mathcal{L}_2, \qquad (14)$$

where $\alpha_1$ and $\alpha_2$ are hyper-parameters.

# 3 Experiments

## 3.1 Datasets

We conduct experiments on the benchmark DSTC4 (Kim et al., 2017b), which consists of 31,034 utterances of human-human multi-turn dialogues on touristic information for Singapore and are divided into 35 sessions. We adopt the same dataset partition in the DSTC4 main task and we regard its speech act attributes as intents.[2] It has 12,759 utterances for training, 4,812 utterances for validation and 7,848 utterances for test.

---

[2]The official DSTC4 pilot tasks' Handbook http://www.colips.org/workshop/dstc4/DSTC4_pilot_tasks.pdf

To justify the generalization of the proposed model, we construct another multi-intent SLU dataset (MixSNIPS). MixSNIPS dataset is collected from the Snips personal voice assistant. To simulate the utterances with multi-intent in the real-world scenarios, we use conjunctions, *e.g.*, "and", to connect sentences with different intents and ensure that the ratio of sentences has 1-3 intents is $[0.3, 0.5, 0.2]$. Finally, we get the 45,000 utterances for training, 2,500 utterances for validation and 2500 utterances for test on MixSNIPS dataset.

In addition, we also conduct experiments on two public benchmark single-intent dataset to validate the efficiency of our proposed model. One is the ATIS dataset (Hemphill et al., 1990) and the other is SNIPS dataset (Coucke et al., 2018), which are widely used as benchmark in SLU research. Both datasets follow the same format and partition as in Goo et al. (2018).

## 3.2 Experimental Settings

The dimension of the word embedding is 64 and the self-attentive encoder hidden units is 256 in all datasets. L2 regularization $1 \times 10^{-6}$ and dropout rate 0.5 are adopted in our model for reducing overfitting. We use Adam (Kingma and Ba, 2014) to optimize the parameters in our model and adopted the suggested hyper-parameters for optimization. For all the experiments, we select the model which works the best on the dev set, and then evaluate it on the test set.

## 3.3 Baselines

We first compare our model with the existing multi-intent SLU state-of-the-art baseline **Joint Multiple ID-SF**. Gangadharaiah and Narayanaswamy (2019) proposes an attention-based model to perform multi-intent classification at both the sentence-level and the token-level. Then, we compare our framework with the existing state-of-the-art single-intent SLU baselines including: 1) **Attention BiRNN.** Liu and Lane (2016) proposes an alignment-based RNN with the attention mechanism, which implicitly learns the relationship between slot and intent. 2) **Slot-Gated Atten.** Goo et al. (2018) proposes a slot-gated joint model to explicitly consider the correlation between slot filling and intent detection. 3) **Bi-Model.** Wang et al. (2018) proposes the Bi-model to consider the cross-impact between the intent detection and slot filling. 4) **SF-ID Network.** Haihong et al. (2019) proposes an SF-ID network to establish direct con-

| Model | DSTC4 | | | | MixSNIPS | | | |
|---|---|---|---|---|---|---|---|---|
| | Slot (F1) | Intent (F1) | Intent (Acc) | Overall (Acc) | Slot (F1) | Intent (F1) | Intent (Acc) | Overall (Acc) |
| Attention BiRNN (Liu and Lane, 2016) | 44.0 | - | 42.1 | 32.6 | 89.4 | - | 94.1 | 62.2 |
| Slot-gated Full (Goo et al., 2018) | 45.0 | - | 42.5 | 32.5 | 87.8 | - | 96.0 | 56.5 |
| Slot-gated Intent (Goo et al., 2018) | 50.2 | - | 40.6 | 31.7 | 87.9 | - | 94.2 | 57.6 |
| Bi-Model (Wang et al., 2018) | 44.6 | - | 41.3 | 30.5 | 86.8 | - | 95.3 | 53.9 |
| SF-ID (Haihong et al., 2019) | 51.4 | - | 41.8 | 33.0 | 89.6 | - | 96.3 | 59.3 |
| Stack-Propagation (Qin et al., 2019) | 52.8 | - | 44.9 | 34.6 | 93.9 | - | 96.4 | 75.5 |
| Joint Multiple ID-SF (Gangadharaiah and Narayanaswamy, 2019) | 48.0 | 37.5 | 39.0 | 29.4 | 91.0 | 98.2 | 95.7 | 66.6 |
| Our model | 53.9* | 40.0* | 46.1* | 35.2* | 94.5* | 98.6* | 96.5* | 76.4* |

Table 1: Slot filling and intent detection results on two multi-intent datasets. The numbers with * indicate that the improvement of our model over all the compared baselines is statistically significant with p <0.05 under the t-test.

nections for the slot filling and intent detection to help them promote each other mutually. 5) **Stack-Propagation.** Qin et al. (2019) adopts a joint model with Stack-Propagation to capture the intent semantic knowledge and perform the token-level intent detection to further alleviate the error propagation.

It's worth noticing that those single-intent models can only handle single intent per utterance. In order to enable single-intent baseline models to handle multiple intents per utterance, we sort the multiple intents in the lexicographical order and connect them with # to get the single multi-intent label. For example, "Please play got the time and add it to the playlist named popular rock" contains two intents "PlayMusic" and "AddToPlaylist", we use "PlayMusic#AddToPlaylistc"as its intent label in the single-intent baseline models. For the *Attention BiRNN*, *Slot-gated Atten*, *SF-ID Network* and *Stack-Propagation*, we run their official source code to obtain the results. For the *Bi-Model* and *Joint Multiple ID-SF*, we re-implemented the models and obtained the results on the same datasets because the original paper did not release their codes.

### 3.4 Results

Following Goo et al. (2018) and Qin et al. (2019), we evaluate the SLU performance of slot filling using F1 score. The performance of intent prediction are evaluated by accuracy and marco F1 score. The sentence-level semantic frame parsing are evaluated by overall accuracy which represents all metrics are right in an utterance. Table 1 shows the experiment results of the proposed models on the DSTC4 and MixSNIPS datasets.

From the results, our framework outperforms Joint Multiple ID-SF baseline by a large margin and achieves the state-of-the-art performance. In the DSTC4 dataset, we achieve 5.9% improvement on Slot (F1) score, 2.5% improvement on Intent (F1), 7.1% improvement on Intent (Acc) and 5.8% improvement on Overall (Acc). In the MixSNIPS

dataset, we achieve 3.5% improvement on Slot (F1) score, 0.4% improvement on Intent (F1), 0.8% improvement on Intent (Acc) and 9.8% improvement on Overall (Acc). This indicates the effectiveness of our dynamic intent-slot graph interaction in multi-intent SLU compared with simply leveraging an overall same intents to guide the slot filling (Joint Multiple ID-SF).

In addition, our framework outperforms the state-of-the-art single-intent model (Stack-Propagation), which further proves our model could make dynamic token-level interaction between intent information and slot filling hidden states to effectively improve the SLU performance. Besides, the single-intent SLU systems may encounter the OOV problem because the output space of the single model's classifier is limited to the labels occurring in the training set. In contrast, this is not a problem for our multi-intent model because we perform the multi-label classification and our model can output all combinations of intents. Though increasing the difficulty of multi-intent prediction, our model still achieves the best results, which again demonstrates the effectiveness of our proposed model.

### 3.5 Analysis

In Section 3.4, significant improvements among all four metrics have been witnessed on both two datasets. However, we would like to know the reason for the improvement. In this section, we first explore the effectiveness of the proposed intent-slot graph interaction layer. Next, we study the effectiveness of the token-level dynamic intent integration mechanism. Finally, we give a graph attention visualization to better understand how the graph-interaction method affects and contributes to the performance. In addition, we conduct experiments on the single-intent datasets to verify the generalization of our proposed model.

| Model | DSTC4 | | | | MixSNIPS | | | |
|---|---|---|---|---|---|---|---|---|
| | Slot (F1) | Intent (F1) | Intent (Acc) | Overall (Acc) | Slot (F1) | Intent (F1) | Intent (Acc) | Overall (Acc) |
| w/o Intent-Slot Graph Interaction Layer | 53.6 | 39.7 | 43.9 | 33.5 | 93.8 | 98.0 | 95.2 | 74.0 |
| w/o Token-Level Dynamic Integration | 53.5 | 37.6 | 45.0 | 34.1 | 93.8 | 98.1 | 95.7 | 73.9 |
| Full Model | **53.9** | **40.0** | **46.1** | **35.2** | **94.5** | **98.6** | **96.5** | **76.4** |

Table 2: Ablation Study on DSTC4 and MixSNIPS Datasets.

### 3.5.1 Effectiveness of Intent-Slot Graph Interaction Layer

In this section, we conduct experiments to verify the effectiveness of the proposed intent-slot graph interaction layer. Instead of adopting the GAT to model the interaction between the predicted intents and slot, we utilize the attention mechanism to incorporate the intents information for slot filling at token-level. After obtaining the context intent vector, we sum the vector and the hidden state of slot filling decoder to get the final slot prediction. The results are shown in the first row of Table 2. We can see that our framework outperforms the simple attention aggregation mechanism. We attribute it to the fact that multi-layer graph attention network can automatically capture relevant intents information and better aggregate intents information for each token slot prediction.

### 3.5.2 Effectiveness of Token-Level Dynamic Intent-Slot Integration Mechanism

In this section, we study the effectiveness of the proposed token-level dynamic multiple intents information integration for slot prediction. We conduct experiments by statically providing the same intents for all tokens slot prediction where we sum the predicted intent embeddings and directly add it to the hidden state of slot filling decoder. The result is shown in the second row of Table 2. We can observe that if we only provide an overall intent information for slot filling, we obtain the worse results, which demonstrates the effectiveness of dynamically incorporating intent information at token-level. We believe the reason is that providing the same intents for all tokens can cause the ambiguity where each token is hard to extract the relevant intent information while our dynamic intent integration mechanism can make the model to capture the related intent information to guide the slot prediction.

### 3.5.3 Visualization of Dynamic Graph Interaction Layer

In this section, with the attempt to better understand what the intent-slot graph interaction layer has
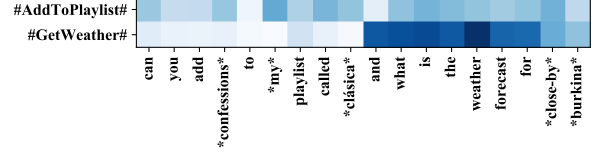


Figure 3: Visualization of the attention weights of slot filling hidden states node in the output head of Dynamic Graph Interaction Layer. Y-axis is the predicted intents and X-axis is the input utterance where slot tokens are surrounded by ∗. For each column, the darker the color, it means that the model suggests that this corresponding intent of the row is more relevant, so that it integrates more information from this intent node features.

learnt, we visualize the intents attention weights of slot filling hidden states node in the output head of intent-slot graph interaction layer, which is shown in Figure 3. Based on the utterance "*can you add confessions to my playlist called clsica and what is the weather forecast for close-by burkina*" and the intents "AddToPlaylist" and "GetWeather", we can clearly see the attention weights successfully focus on the correct intent, which means our graph interaction layer can learn to incorporate the correlated intent information at each slot. More specifically, our model properly aggregates the corresponding "AddToPlaylist" intent information at slots "*confessions, my, clsica*" and "GetWeather" intent information at slots"*close-by burkina*".

### 3.5.4 Evaluation on the Single-Intent Datasets

We conduct experiments on two public single-intent benchmark to evaluate the generalizability of the proposed framework. We compare our model with the single-intent state-of-the-art models including **SF-ID**, **Stack-Propagation** and multi-intent model including **Joint Multiple ID-SF**. Table 3 shows the experiment results of the proposed models on the ATIS and SNIPS datasets. From the table, we can see that our model significantly outperforms all the compared baselines and achieves the state-of-the-art performance. We obtain 0.7% improvement on Overall (Acc) and 0.4% improve-

| Model | ATIS | | | | SNIPS | | | |
|---|---|---|---|---|---|---|---|---|
| | Slot (F1) | Intent (F1) | Intent (Acc) | Overall (Acc) | Slot (F1) | Intent (F1) | Intent (Acc) | Overall (Acc) |
| SF-ID (Haihong et al., 2019) | 95.6 | - | 96.6 | 86 | 90.5 | - | 97 | 78.4 |
| Stack-Propagation (Qin et al., 2019) | 95.9 | - | 96.9 | 86.5 | 94.2 | - | 98.0 | 86.9 |
| Joint Multiple ID-SF (Gangadharaiah and Narayanaswamy, 2019) | 94.2 | - | 95.4 | - | 88.0 | - | 97.2 | - |
| Our model | 96.0* | 80.2 | 97.1* | 87.2* | 94.8* | 98.3 | 98.1* | 87.3* |

Table 3: Slot filling and intent detection results on two single-intent datasets. The numbers with * indicate that the improvement of our model over all the compared baselines is statistically significant with p <0.05 under the t-test.

ment on Overall (Acc) on ATIS and SNIPS dataset, respectively. This demonstrates the generalizability and effectiveness of our framework whether handling multi-intent or single-intent SLU.

## 4 Related Work

Our work is related to the following research directions.

**Intent Detection** Intent detection aims to classify user intents given their diversely expressed utterances in the natural language and is formulated as an utterance classification problem. Different classification methods, such as support vector machine (SVM) and RNN (Haffner et al., 2003; Sarikaya et al., 2011), have proposed to solve it. Xia et al. (2018b) adopts a capsule-based neural network with self-attention for intent detection. However, the above models mainly focus on the single intent scenario, which can not handle the complex multiple intent scenario. Recently, Xu and Sarikaya (2013b) and Kim et al. (2017a) explore the complex scenario, where multiple intents are assigned to a users utterance. Xu and Sarikaya (2013b) use log-linear models to achieve this, while we use neural network models. Compared with their work, we jointly perform multi-label intent classification and slot prediction, while they only consider intents and do not perform slot prediction.

**Slot Filling** Slot filling can be treated as a sequence labeling task, and the popular approaches are conditional random fields (CRF) (Raymond and Riccardi, 2007) and recurrent neural networks (RNN) (Xu and Sarikaya, 2013a; Yao et al., 2014). Recently, Shen et al. (2018) and Tan et al. (2018) introduce the self-attention mechanism for CRF-free sequential labeling. Recent state-of-the-art model (Goo et al., 2018; Li et al., 2018; Xia et al., 2018a; Qin et al., 2019; E et al., 2019; Liu et al., 2019) adopt the joint model to incorporate intent information for slot filling.

**Joint Model** To consider the high correlation between intent and slots, many joint models are proposed to solve two tasks simultaneously in a

unified framework. Goo et al. (2018); Li et al. (2018); Zhang et al. (2019); Qin et al. (2019) propose to utilize the intent information to guide the slot filling. Wang et al. (2018); E et al. (2019) consider the cross-impact between the slot and intents. Our framework follows those state-of-the-art joint model paradigm, and further focus on the multiple intents scenario while the above joint model does not consider. Recently, Gangadharaiah and Narayanaswamy (2019) propose a joint model to consider the multiple intent detection and slot filling simultaneously where they explicitly leverage an overall intent information with gate mechanism to guide all tokens slot prediction. Compared with this work, the main differences are as following: 1) Our framework exploits the interaction between multiple intents and slot in a unified graph architecture, making a fine-grained intent information transfer for token-level slot prediction while their work simply incorporates the same intents information for all tokens slot prediction. To our best of knowledge, this is the first work to explore fine-grained intent information transfer in multi-intent SLU. 2) As far as we know, their corpus and code are not distributed, which makes it hard to follow. In contrast, we empirically construct a large-scale multi-intent SLU dataset where all datasets and code will release, where we hope it would push forward the research of multi-intent SLU.

## 5 Conclusion

In our paper, we propose a token-level dynamic graph-interactive network to model the interaction between multiple intents and slot at each token, which can make a fine-grained intent information transfer for slot prediction. To our best of knowledge, this is the first work to explore fine-grained intents information transfer in multi-intent SLU. Experiments on four datasets show the effectiveness of the proposed models and achieve the state-of-the-art performance. In addition, we empirically construct a large-scale multi-intent SLU dataset. The release of it would push forward the research of multi-intent SLU.

# References

Alice Coucke, Alaa Saade, Adrien Ball, Théodore Bluche, Alexandre Caulier, David Leroy, Clément Doumouro, Thibault Gisselbrecht, Francesco Caltagirone, Thibaut Lavril, et al. 2018. Snips voice platform: an embedded spoken language understanding system for private-by-design voice interfaces. *arXiv preprint arXiv:1805.10190*.

Haihong E, Peiqing Niu, Zhongfu Chen, and Meina Song. 2019. A novel bi-directional interrelated model for joint intent detection and slot filling. In *Proc. of ACL*.

Rashmi Gangadharaiah and Balakrishnan Narayanaswamy. 2019. Joint multiple intent detection and slot labeling for goal-oriented dialog. In *Proc. of NAACL*, pages 564–569.

Chih-Wen Goo, Guang Gao, Yun-Kai Hsu, Chih-Li Huo, Tsung-Chieh Chen, Keng-Wei Hsu, and Yun-Nung Chen. 2018. Slot-gated modeling for joint slot filling and intent prediction. In *Proc. of NAACL*.

Patrick Haffner, Gokhan Tur, and Jerry H Wright. 2003. Optimizing svms for complex call classification. In *In Proc. of ICASSP*.

E Haihong, Peiqing Niu, Zhongfu Chen, and Meina Song. 2019. A novel bi-directional interrelated model for joint intent detection and slot filling. In *Proc. of ACL*, pages 5467–5471.

Charles T Hemphill, John J Godfrey, and George R Doddington. 1990. The atis spoken language systems pilot corpus. In *Speech and Natural Language: Proceedings of a Workshop Held at Hidden Valley, Pennsylvania, June 24-27, 1990*.

Sepp Hochreiter and Jürgen Schmidhuber. 1997. Long short-term memory. *Neural computation*, 9(8).

Byeongchang Kim, Seonghan Ryu, and Gary Geunbae Lee. 2017a. Two-stage multi-intent detection for spoken language understanding. *Multimedia Tools and Applications*, 76(9):11377–11390.

Seokhwan Kim, Luis Fernando DHaro, Rafael E Banchs, Jason D Williams, and Matthew Henderson. 2017b. The fourth dialog state tracking challenge. In *Dialogues with Social Robots*, pages 435–449. Springer.

Diederik P Kingma and Jimmy Ba. 2014. Adam: A method for stochastic optimization. *arXiv preprint arXiv:1412.6980*.

Changliang Li, Liang Li, and Ji Qi. 2018. A self-attentive model with gate mechanism for spoken language understanding. In *Proc. of EMNLP*.

Bing Liu and Ian Lane. 2016. Attention-based recurrent neural network models for joint intent detection and slot filling. *arXiv preprint arXiv:1609.01454*.

Yijin Liu, Fandong Meng, Jinchao Zhang, Jie Zhou, Yufeng Chen, and Jinan Xu. 2019. Cm-net: A novel collaborative memory network for spoken language understanding. *arXiv preprint arXiv:1909.06937*.

Libo Qin, Wanxiang Che, Yangming Li, Haoyang Wen, and Ting Liu. 2019. A stack-propagation framework with token-level intent detection for spoken language understanding. In *Proc. of EMNLP*.

Christian Raymond and Giuseppe Riccardi. 2007. Generative and discriminative algorithms for spoken language understanding. In *Eighth Annual Conference of the International Speech Communication Association*.

Ruhi Sarikaya, Geoffrey E Hinton, and Bhuvana Ramabhadran. 2011. Deep belief nets for natural language call-routing. In *ICASSP*.

Sebastian Schuster, Sonal Gupta, Rushin Shah, and Mike Lewis. 2019. Cross-lingual transfer learning for multilingual task oriented dialog. In *Proc. of NAACL*.

Tao Shen, Tianyi Zhou, Guodong Long, Jing Jiang, Shirui Pan, and Chengqi Zhang. 2018. Disan: Directional self-attention network for rnn/cnn-free language understanding. In *Proc. of AAAI*.

Zhixing Tan, Mingxuan Wang, Jun Xie, Yidong Chen, and Xiaodong Shi. 2018. Deep semantic role labeling with self-attention. In *Proc. of AAAI*.

Gokhan Tur and Renato De Mori. 2011. *Spoken language understanding: Systems for extracting semantic information from speech*. John Wiley & Sons.

Ashish Vaswani, Noam Shazeer, Niki Parmar, Jakob Uszkoreit, Llion Jones, Aidan N Gomez, Ł ukasz Kaiser, and Illia Polosukhin. 2017. Attention is all you need. In *NIPS*.

Petar Veličković, Guillem Cucurull, Arantxa Casanova, Adriana Romero, Pietro Lio, and Yoshua Bengio. 2017. Graph attention networks. *arXiv preprint arXiv:1710.10903*.

Yu Wang, Yilin Shen, and Hongxia Jin. 2018. A bi-model based rnn semantic frame parsing model for intent detection and slot filling. In *Proc. of ACL*.

Congying Xia, Chenwei Zhang, Xiaohui Yan, Yi Chang, and Philip Yu. 2018a. Zero-shot user intent detection via capsule neural networks. In *Proc. of EMNLP*.

Congying Xia, Chenwei Zhang, Xiaohui Yan, Yi Chang, and Philip Yu. 2018b. Zero-shot user intent detection via capsule neural networks. In *Proc. of EMNLP*, pages 3090–3099, Brussels, Belgium. Association for Computational Linguistics.

Puyang Xu and Ruhi Sarikaya. 2013a. Convolutional neural network based triangular crf for joint intent detection and slot filling. In *2013 IEEE Workshop on Automatic Speech Recognition and Understanding*.

Puyang Xu and Ruhi Sarikaya. 2013b. Exploiting shared information for multi-intent natural language sentence classification. In *INTERSPEECH*.

Kaisheng Yao, Baolin Peng, Yu Zhang, Dong Yu, Geoffrey Zweig, and Yangyang Shi. 2014. Spoken language understanding using long short-term memory neural networks. In *SLT*.

Steve Young, Milica Gašić, Blaise Thomson, and Jason D Williams. 2013. Pomdp-based statistical spoken dialog systems: A review.

Chenwei Zhang, Yaliang Li, Nan Du, Wei Fan, and Philip Yu. 2019. Joint slot filling and intent detection via capsule neural networks. In *Proc. of ACL*.

Victor Zhong, Caiming Xiong, and Richard Socher. 2018. Global-locally self-attentive encoder for dialogue state tracking. In *Proc. of ACL*.